IEEE Access
Multidisciplinary | Rapid Review | Open Access Journal

Received October 3, 2018, accepted October 16, 2018, date of publication October 22, 2018, date of current version November 14, 2018.

Digital Object Identifier 10.1109/ACCESS.2018.2876872

A Compact Multi-Beam End-Fire Circularly Polarized Septum Antenna Array for Millimeter-Wave Applications

XIAOHE CHENG[1,2], (Student Member, IEEE), YUAN YAO[1], (Senior Member, IEEE), TAKASHI TOMURA[2], (Member, IEEE), JIRO HIROKAWA[2], (Fellow, IEEE), TAO YU[2], JUNSHENG YU[1], (Senior Member, IEEE), AND XIAODONG CHEN[3], (Fellow, IEEE)

[1]Beijing Key Laboratory of Work Safety Intelligent Monitoring, School of Electronic Engineering, Beijing University of Posts and Telecommunications, Beijing 100876, China
[2]Department of Electrical and Electronic Engineering, Tokyo Institute of Technology, Tokyo 152-8552, Japan
[3]School of Electronic Engineering and Computer Science, Queen Mary University of London, London E1 4NS, U.K.

Corresponding author: Yuan Yao (yaoy@bupt.edu.cn)

This work was supported in part by the National Natural Science Foundations of China under Grant 61474112, in part by the BUPT Excellent Ph.D. Students Foundation under Grant CX2017304, and in part by the China Scholarship Council.

ABSTRACT In this paper, a novel circularly polarized end-fire septum antenna based on substrate-integrated-waveguide (SIW) is proposed in the 60-GHz band. By introducing four symmetrical tapered curved air slots in three stacked open-ended SIW layers, the antenna can obtain an operating bandwidth from 57.2 to 63.4 GHz for both AR < 3 dB and $|S_{11}| < -21$ dB. Besides, the half-power-beam-width and 3-dB axial-ratio (AR) beam-width are all wider than 79°, and a stable gain of 7.57 dBic with a variation of 0.15 dBic can be achieved in the working band. A 4×4 SIW Butler matrix based on SIW with three same substrates is then designed. The modified two-layer phase shifters realized by the different path distance are employed in the folded Butler matrix. By combining the antenna element and the Butler matrix together, a four-beam antenna array with circular polarization wave is realized. The proposed array has been fabricated and measured. The measurement results show that the antenna gain up to 11.01 dBic, -10 dB impedance and isolation bandwidth from 57.8 to 62.5 GHz (except at around 58.3 GHz), stable radiation pattern and a wide angular range of $\pm 37°$ can be obtained. The measured AR values of the main lobe range of four beams are all less than 5 dB from 58 to 60 GHz.

INDEX TERMS Butler matrix, circularly polarized, end-fire, millimeter wave, multi-beam, substrate integrated waveguide.

I. INTRODUCTION

Millimeter-wave (MMW) technology has been attracting much attention to realize the upcoming 5th-generation mobile networks [1]. It is widely known that the electromagnetic wave suffers from higher space loss and blockage effects at MMW band than microwave band, which substantially deteriorates the coverage and the signal-to-noise ratio (SNR) [2]. The high gain antenna array with narrow beam width is a reasonable solution to address this shortcoming [3]. To enlarge the spatial coverage without increasing the interference, multi-beam antenna arrays with passive beam-forming networks (BFNs), which have ability to cover a predetermined angular range with independent high gain beams and avoid the inter-connection/cell interference due to the narrow beam-width, receive extensive attention [5], [6]. As one of the most popular BFNs, the Butler matrix based on SIW is a strong candidate for MMW multi-beam antenna due to its relatively low transmission loss and low processing cost [7]–[9]. Recently, the multi-folded Butler matrixes based on SIW have been proposed in [10] and [11], which can achieve a more compact size than the traditional one.

The circularly polarized (CP) antenna has advantages of providing a flexible orientation angle between transmitting and receiving antennas, and it can reduce the multipath effects in contrast to the linearly polarized (LP) antennas [12], [13]. However, there are only a few research working on the MMW CP multi-beam array. A broadside multi-beam array with multiple polarizations was proposed in [14], but the axial-ratio (AR) value of the radiation pattern would deteriorate significantly in the outside direction

2169-3536 © 2018 IEEE. Translations and content mining are permitted for academic research only.
Personal use is also permitted, but republication/redistribution requires IEEE permission.
See http://www.ieee.org/publications_standards/publications/rights/index.html for more information.

beam due to the narrow 3-dB AR beam width of the radiation element. A stacked curl element with wide AR beam width and operating bandwidth based on SIW was proposed in [15], which is suitable for broadside multi-beam array applications.

For the purpose of enriching the radiation direction of the multi-beam antenna array, the array with end-fire radiation pattern would be more promising in the portable devices due to its ability to save the space occupied by antenna element and to avoid the undesirable interference from user's hand on antenna radiation characteristic as much as possible [16] and [17]. It plays a vital role to select an antenna element in building a CP end-fire multi-beam array due to its decisive effects on the performance of the array. Antenna element should meet three conditions: symmetrically wide half power beam width (HPBW), wide 3-dB AR beam width and narrow structure width. However, there are not many studies on end-fire CP antenna. The CP tapered slot antennas based on waveguide with wide operating bandwidth were proposed in [18] and [19]. However, the aperture width of this type CP antenna is too large to be employed as a multi-beam antenna element, even in the compact version based on ridge waveguide [20]. The CP septum antenna with wide 3-dB AR beam width operating at 60 GHz based on waveguide was proposed in [21], but the aperture width of this antenna is also too large which is equal to the width of WR-15. In addition, its HPBW is narrow, 62° at 60 GHz, which will enlarge the gain variation between different beams in multi-beam array applications. Recently, a dual circularly polarized multi-beam end-fire array using dielectric loaded stepped slot antennas was proposed in [22], which can achieves wide operating bandwidth of 22.5%.

In this paper, to reduce the aperture width and broaden the HPBW of the end-fire CP septum antenna based on waveguide, a septum antenna element designed on three layer SIWs is proposed. Considering various PCB processing constraints such as usable substrate thickness and minimum distance between metal holes and slots, the exponential curve slot is employed to obtain the CP characteristic. The properties difference between the septum antenna based on air-filled waveguide and SIW is explained. Compared with the element in [22], the proposed element can achieve more compact structure in width and length. The width of element can be reduced from 0.75λ to 0.58λ with almost same dielectric constant substrate. Therefore, the lower side lobe level can be achieved. A folded 4 × 4 SIW Butler matrix with simpler two-layered phase shifters is then designed in same three substrates. By employing the antenna elements and Butler matrix, a four-beam CP antenna array is simulated and measured.

The remaining parts of this paper are organized as follows. The configuration and the operating principle of the antenna element are presented in Section II; the details of the 4 × 4 Butler matrix is described in section III; Section IV discuss the simulation and measurement of the CP multi-beam array. And in Section V, the conclusion is summarized.

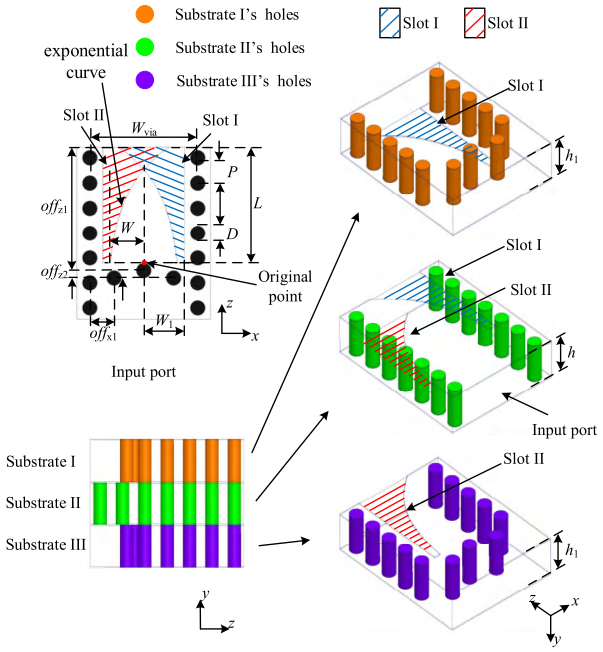

FIGURE 1. Configuration of the proposed septum antenna element based on SIW.

II. SEPTUM ANTENNA ELEMENT

A. CONFIGURATION

The geometry of the proposed CP septum antenna element based on SIW is illustrated in Fig. 1, wherein the whole structure is realized in three stacked printed circuit board (PCB) substrates. As shown in Fig. 1, the metallic holes of SIW in different substrate layers are distinguished by different colors. The positions of the holes are given in the x-z plane in Fig. 1. The symmetrical air slots in the copper coating of the PCB substrates are covered by blue and red lines. The blue slots are located in the bottom and top layers in the Substrate I and Substrate II, respectively. And the red ones are in the bottom and top layers in the Substrate II and Substrate III, respectively. The slot employs one exponential curve and a linear line as a combination. Since the Slot I and Slot II are symmetric, we describe the slot II only. As origin of coordinate are specified in Fig. 1, the curve can be determined by the following function,

$$x(z) = \frac{e^{Qz} - 1}{k} - W \tag{1}$$

where the argument z varies from 0 to L. According to Eq.(1), the values of Q and k decide the curvature of the curve, and the value of W controls the starting point of the curve. The linear line extending from point $(-W_1, 0)$ are parallel to z axis. In this design, all substrates are NPC-H220A (processed by Nippon Pillar Packing Co., Ltd.) with thickness of 1.2 mm, dielectric constant of 2.18 and dielectric loss tangent of 5×10^{-4}. The thickness and conductivity of copper clad are set to 0.035 mm and 5.8×10^7 in simulation, respectively. The accurate dimensions of the antenna are given in Table 1.

TABLE 1. Dimension of CP antenna element (units: mm).

Parameters	W_{via}	P	D	L	W	W_1
Values	2.9	0.67	0.4	3.155	0.9	1.1
Parameters	off_{z1}	off_{z2}	off_{x1}	Q	k	
Values	3.355	3.555	0.65	0.84	8	

B. OPERATING PRINCIPLE

The operating mechanism of the septum antenna based on waveguide has been explained in [21]. The SIW transmission line has similar working mechanism with air-filled waveguide. Therefore, the CP wave generation principle of the proposed antenna based on SIW will not be explained again in this paper. However, by replacing the air with the high dielectric substrate, the radiation performance of the septum antenna will be changed obviously.

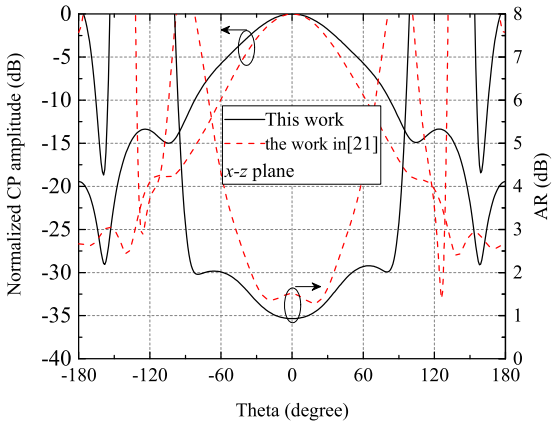

FIGURE 2. Simulated CP radiation patterns and AR plots in x-z and y-z plane of the septum antenna based on air-filled waveguide [21] and SIW (this work). (a) x-z plane. (b) y-z plane.

The HPBW of the reference antenna based on air-filled waveguide is too narrow to be employed in the multi-beam array element design. Filling with high dielectric constant in waveguide can be used to reduce the aperture size of the antenna, which can reduce the directivity and broaden the HPBW. Fig. 2 compares the CP radiation patterns of the

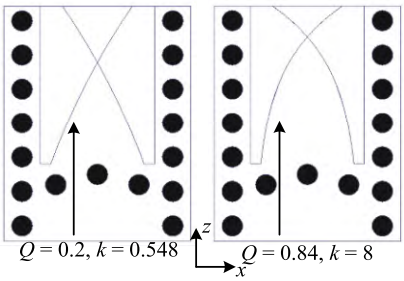

FIGURE 3. Proposed antenna element with different slot curve parameters.

structure based on waveguide [21] and this design. It should be noted that the structure parameters of the reference antenna are kept the same as given in [21]. Fig. 2 shows that the HPBW can increase from 62° to 80° in x-z plane at 60 GHz. The AR beam width is also enlarged from 76° to 177°. Besides, in y-z plane, the AR beam width increases from 94° to 172°, while the HPBW maintains at 68°. As explained in [21], the width of the y-direction antenna aperture will have influence on phase and amplitude differences of x- and y-direction electric field in the far field (Ex and Ey). Therefore, this width is an important optimization parameter for the septum antenna to obtain CP radiation characteristics. However, it is difficult to realize in SIW structure due to limited available substrate thickness. In order to overcome the issue, the exponential curve slot is developed. As shown in Fig. 3, two sets of curve parameters (($Q = 0.84$, $k = 8$) and ($Q = 0.2$, $k = 0.548$)) determine two slots with curve and approximate linear line, respectively. The phase and amplitude differences of Ex and Ey of these two sets of parameters are illustrated in Fig. 4. The amplitudes of Ex and Ey obviously increase and decrease with increase in the curvature of the slot, respectively, which can be used to optimize the amplitude difference required for CP characteristics. The curvature of curve also determines the position of coupling strength, which affects the phase difference as shown in Fig. 4. Therefore, employing the exponential curve slot can increase optimization space for the septum antenna to achieve CP characteristic.

The simulated AR, $|S_{11}|$ and left hand circular polarization (LHCP) gain of the proposed antenna element at $+z$-direction are illustrated in Fig. 5. Simulation results show that the element can achieve an operating bandwidth from 57.2 to 63.4 GHz for both AR < 3 dB and $|S_{11}| < -21$dB. A stable gain of 7.57 ± 0.15 dBic is achieved in the overall bandwidth. It should be noted that the AR bandwidth of the proposed antenna is obviously narrower than the work in [21]. As shown in Fig. 6, when the electromagnetic wave radiates from antenna aperture to the air, a part of power of the incident wave will be reflected on the substrate-air interface due to the abrupt changes of dielectric constant. The reflected wave will be radiated again by the antenna and be added to the incident wave. The phase of the reflected wave will be changed with the frequency. Therefore, the amplitude

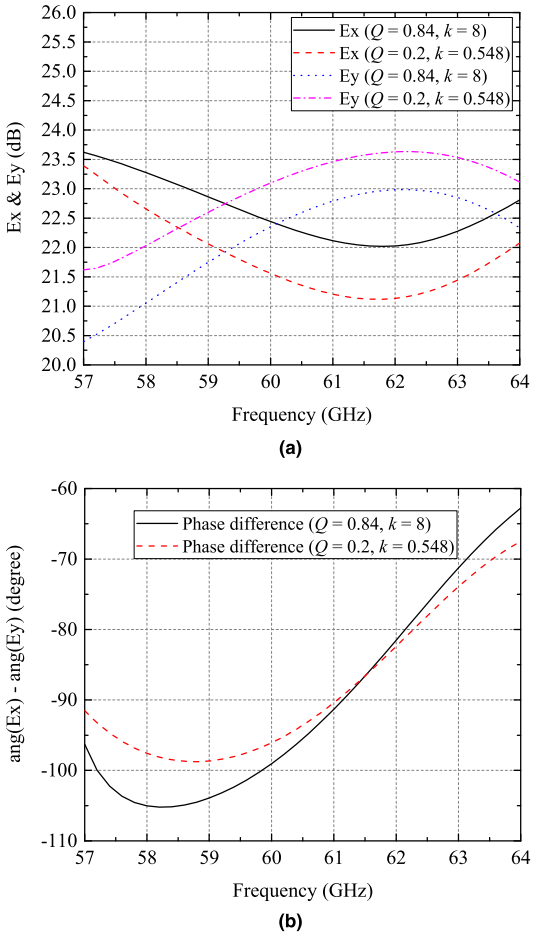

FIGURE 4. Simulated amplitude and phase of Ex and Ey in the far field of the proposed antenna element with different slot curve parameters. (a) Amplitude. (b) Phase difference.

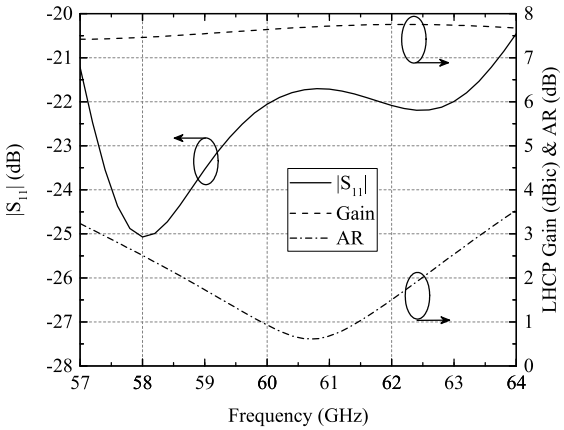

FIGURE 5. Simulated $|S_{11}|$, LHCP Gain, and AR plots at $+z$ direction of the proposed antenna element.

and phase differences of Ex and Ey cannot maintain stable within the very wide frequency band. The AR beam width and HPBW with frequency from 57.2 to 63.4 GHz in x-z plane are presented in Fig. 7, from which it can be seen that the wide HPBWs with 79.45° ± 1.15° and the wider 3-dB AR

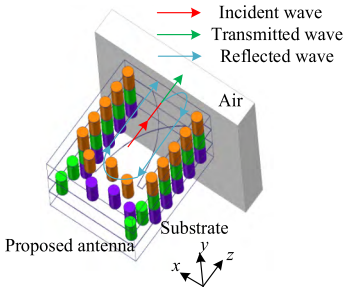

FIGURE 6. Radiation mechanism of the proposed antenna element.

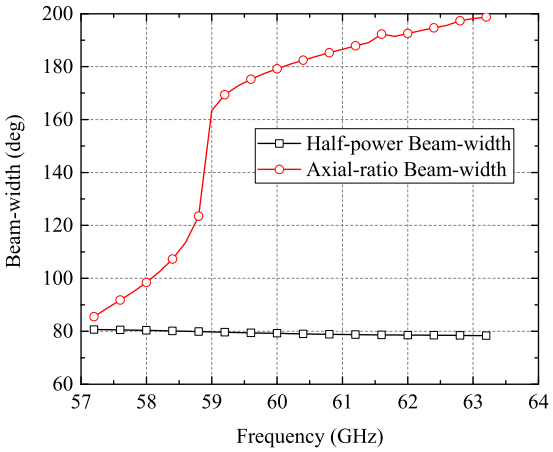

FIGURE 7. Simulated HPBW and AR beam-width in x-z plane of the proposed antenna element.

beam widths are achieved, and this prepared the ground for multi-beam array with good polarization purity.

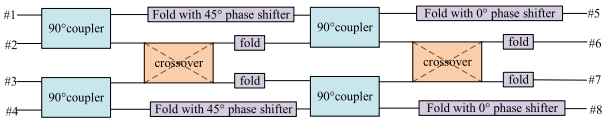

FIGURE 8. Block diagram of the 4 × 4 folded Butler matrix.

III. 4 × 4 BUTLER MATRIX

The folded Butler matrix based on SIW is an effective and economic choice for realizing the passive MMW multi-beam antenna array with a compact size, and has been studied in [10] and [11]. Because the CP antenna element is based on three laminates, a folded 4 × 4 Butler matrix with the same three substrates is employed to feed the antenna. The block diagram of the proposed folded Butler matrix is illustrated in Fig. 8, which consists of four 90° couplers, two crossovers and four phase shifters. The final structure of the Butler matrix connected with the proposed CP antenna element is shown in Fig. 9. It should be noted that the color definition of the holes in Fig. 9 is kept the same as defined in Fig. 1, and will be used in all multilayer structure figures in this paper unless otherwise stated.

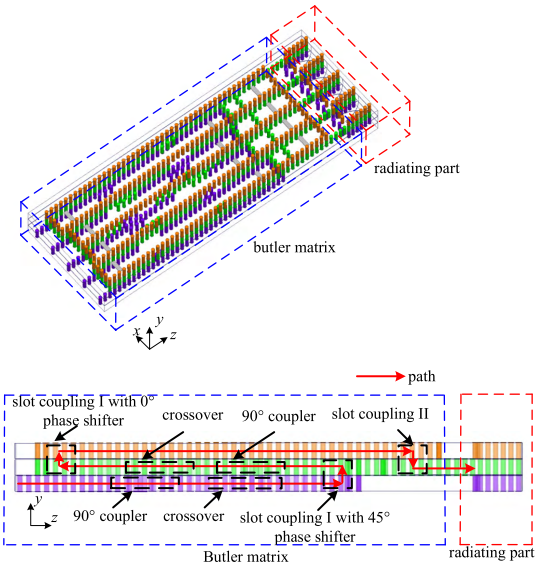

FIGURE 9. Structure of the proposed Butler matrix connected with the element.

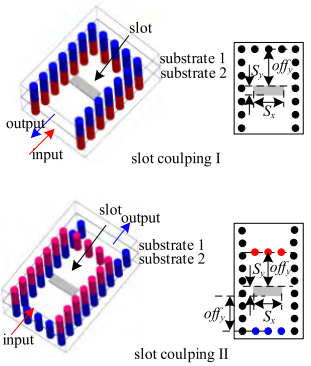

FIGURE 10. Configuration of layer-to-layer transitions.

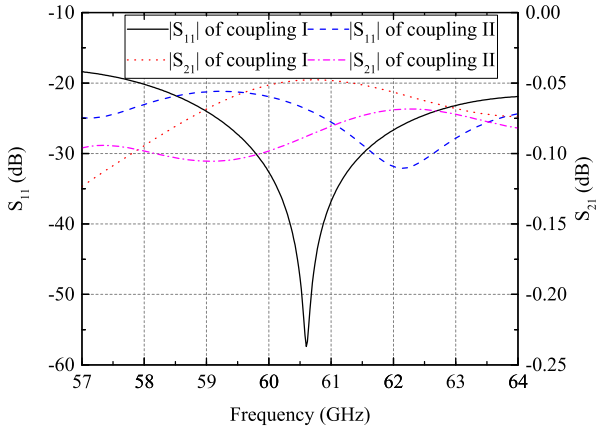

FIGURE 11. Simulated S-parameter of layer-to-layer transitions.

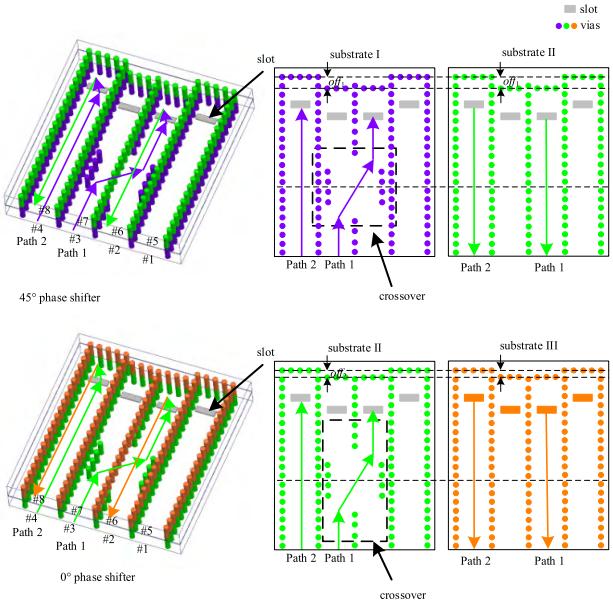

FIGURE 12. Configuration of 45° and 0° phase shifters with crossover.

The 90° coupler and crossover reported in [17] are employed in this design. Because the Butler matrix is folded, 0° and 180° layer-to-layer transition named slot coupling I and II are needed. As shown in Fig. 10, the slots with length of S_x and width of S_y are placed between the two laminate. Two short-ended SIW sections with offset of off_y are placed in the adjacent substrate. It should be noted that the colors of the holes in Fig. 10 are only used to distinguish different layers. The detail values of the dimension are presented in Table 2, from which it can be seen that the $|S_{11}|$ of the two bends are all less than -18 dB from 57 to 64 GHz as shown in Fig. 11.

TABLE 2. Dimension of layer-to-layer transitions (Units: mm).

Parameters	S_x	S_y	off_y
Values	1.57	0.49	1.95

As we know, the SIW transmission lines are composed of metallic holes. Because the metalized holes process need to keep some distance between two adjacent holes, designing the phase shifter reported in [11] and [17] has more optimized parameters than metal waveguide. In this design, a simpler phase shifter structure is proposed as shown in Fig. 11. The phase shift is realized by the different path distance of Path 1 and Path 2 as marked in Fig. 12. It is rapid and precise to optimize the 0° and 45° phase shifter. Considering the slot coupling I as a whole, therefore there is only one parameter (off_1 or off_2) to be optimized to obtain the 45° or 0° phase shift needed for Butler matrix. The simulated phase responses of the phase shifters (characterized by ∠S63-∠S84) as defined in Fig.12) are given in Fig. 13. The phase error of the 0° and 45° phase shifter are less than ±2.7° and ±8.1° from 57 to 64 GHz, respectively.

By arranging the components mentioned above according to the law shown in Fig. 8, a 4 × 4 Butler matrix can be obtained. For the sake of integration with the proposed antenna element, the slot coupling II is employed to

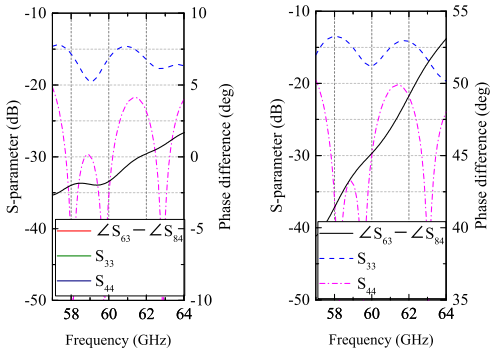

FIGURE 13. Simulated S-parameters and phase difference of the 45° and 0° phase shifter.

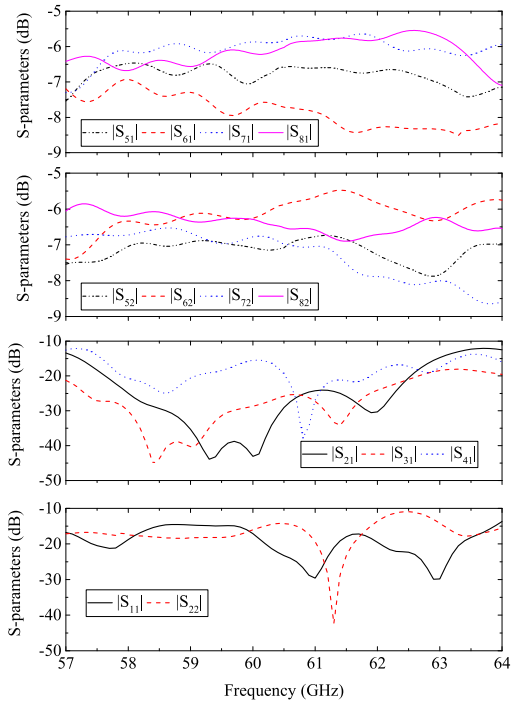

FIGURE 14. Simulated S-parameters of the proposed Butler matrix.

transfer the electromagnetic wave from top layer to middle layer as defined in Fig. 9. Due to the symmetry of the Butler matrix, the $|S_{11}|$ and $|S_{22}|$ are the same with the $|S_{33}|$ and $|S_{44}|$, respectively. The simulated S-parameters and phase responses of the folded Butler matrix are presented in Fig. 14 and Fig. 15, respectively. The simulated reflection coefficient and isolation of the Butler matrix are all less than −10 dB. The magnitude and phase errors which are less than ±1.5 dB and ±19° for all ports can be achieved from 57 GHz to 64 GHz, respectively.

IV. FOUR-BEAM END-FIRE ARRAY

The photograph of the three-layered 1 × 4 CP multi-beam antenna array fabricated by PCB facilities is given in Fig. 16. The adhesive (provided by Nippon Pillar Packing Co., Ltd.) with thickness of 0.038mm, dielectric constant of 2.35 and

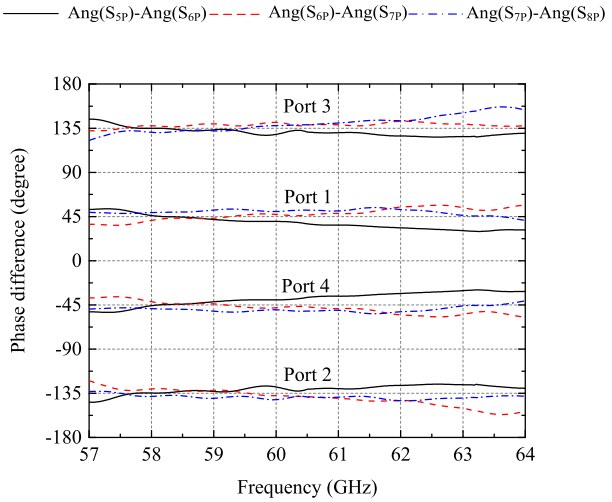

FIGURE 15. Simulated phase difference of the proposed Butler matrix. (ports defined in Fig. 8).

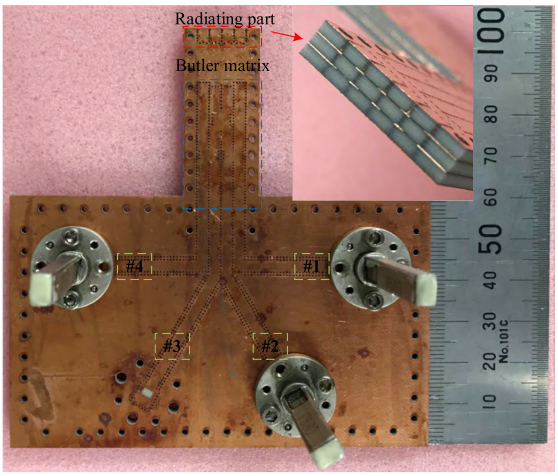

FIGURE 16. Photographs of the fabricated multi-beam antenna array.

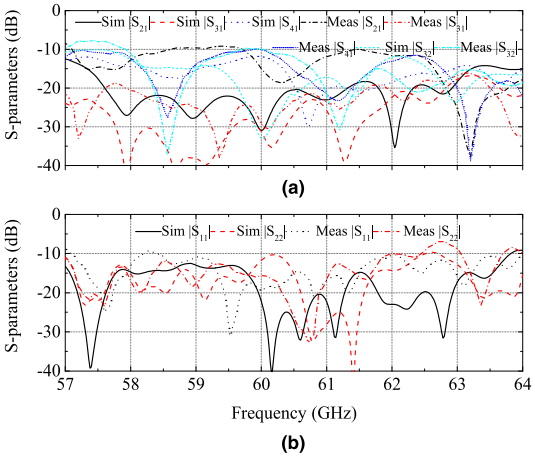

FIGURE 17. Simulated and measured S-parameters of the proposed multi-beam antenna array. (a) isolation. (b) reflection coefficient.

dielectric loss tangent of 2.5×10^{-3} is used for bonding the layers. The element spacing of the antenna array is set as 2.9 mm (0.58 λ at 60 GHz). To measure the performance

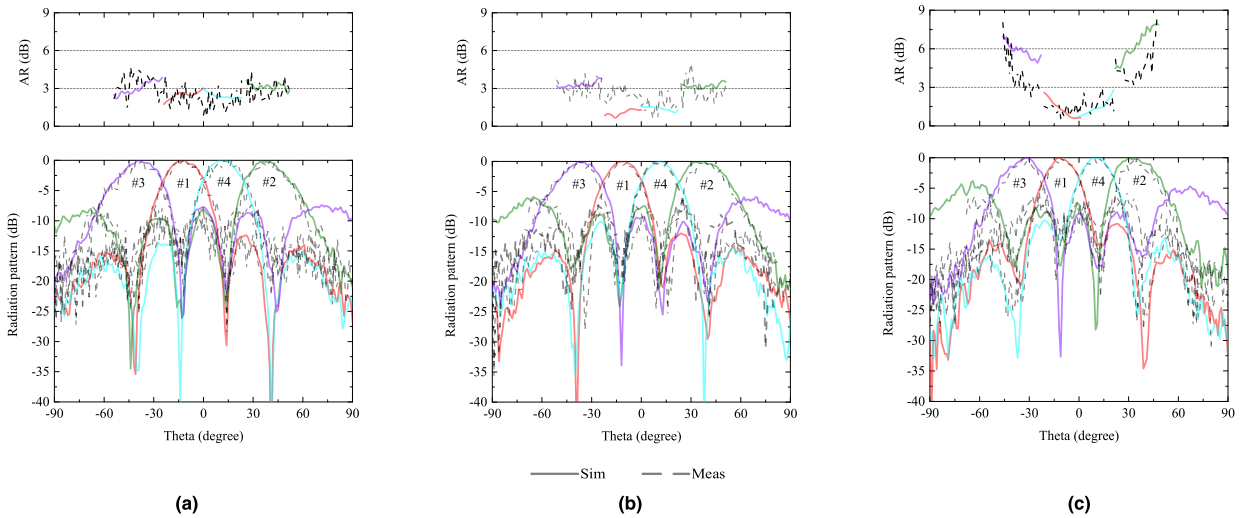

FIGURE 18. Simulated and measured normalized radiation patterns and AR plots in *x-z* plane of the proposed multi-beam antenna array. (a) 58 GHz. (b) 60 GHz. (c) 63 GHz.

of the array, the SIW to WR-15 transition is designed for each input port. Comparisons between the simulation and the measurement results are given in the following. All the simulations are done with full-wave electro-magnetic solver Ansoft HFSS. In measurement, the ports that were not under test were connected with WR-15 waveguide loads.

Due to the symmetry of the array configuration, the S-parameter of port3 and port4 should be the same with port1 and port2. Fig. 17 shows the simulated and measured impedance and isolation performances of the proposed array. The simulated overlapped bandwidth of input ports is from 57 to 63.8 GHz for S-parameter less than −10 dB, and the measured one is covered from 57.8 GHz to 62.5 GHz (except at around 58.3 GHz). The higher value in measurement is mainly caused by the fabrication tolerance, such as increasing surface roughness caused by the various possible unwanted scratches occur on the cladding, position offset of each stacked substrate, and cutting error of the radiating aperture of array as shown in the enlarged section diagram of radiation part in Fig. 16.

The simulated and measured four beams generated by the proposed CP array at 58, 60, and 63 GHz in *x-z* plane are given in Fig. 18 with solid and dash line, respectively. In the far field measurement setup to test the LHCP radiation pattern, the transmitting antenna is set as a horn antenna for horizontal and vertical polarization. The radiation patterns are calculated by the superposition of these two measurement results. The AR value is calculated by comparing the maximum received power with the minimum one of a rotated linearly polarized horn. With reference to Fig. 18, the main beams in simulations and measurements agree well with each other. The unsmooth measured result is caused by the air gap between the adjacent substrates introduced by the surface roughness of the copper clad. The measured results are incomplete due to the limit of the rotation range

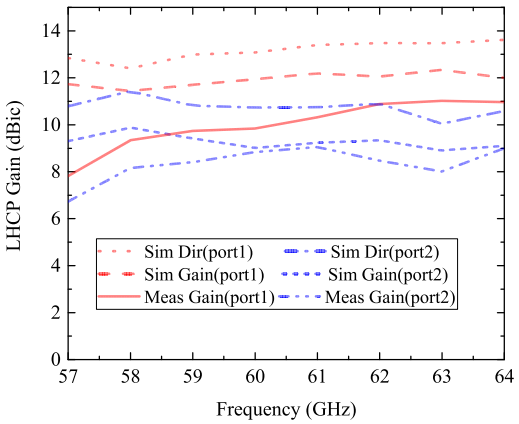

FIGURE 19. Simulated LHCP gains and directivities and measured LHCP gain of the proposed multi-beam antenna array.

of revolving stage. The four beams can cover an azimuthal range of ±37°. The little difference of side lobe level between simulations and measurements are also mainly caused by the fabrication tolerance. The simulated and measured AR values of the main lobe range of four beams at 60 GHz are all less than 4 dB and are all less than 5 dB from 58 GHz to 60 GHz. The AR value is obviously larger than 3 dB at 63 GHz which is caused by the phase error introduced by the Butler matrix. Fig. 19 presents the simulated gain and directivity and measured directivity of the array when port 1 and 2 are excited, respectively. The simulated directivities of the proposed antenna for feeding from port1 and port2 are around 13 and 10.5 dBic. The simulated gains are around 11.5 and 9.5 dBic for port1 and port2, respectively. The attenuation around 1.5 dBic in measured gain results are mainly caused by the randomly distributed air gap introduced by the increasing surface roughness of cladding of stacked

substrates in fabricated prototype [23]. By comparing the results of simulated directivity and measured gain, the measured radiation efficiency of the array is approximately 50%. The simulated and measured gains variation of each beam are all less than 2.7 dBic from 58 to 63 GHz.

V. CONCLUSION

A CP septum antenna based on three-layer SIW with end-fire radiation, AR and impedance bandwidth from 57.2 to 63.4 GHz, wide AR beam-width larger than 85° in horizontal plane and gain of 7.57 ± 0.15 dBic has been proposed. Then a folded 4×4 Butler matrix designed on same three substrates has also been employed to feed the antenna element. By combining the elements and the beam-forming network, a 1×4 array that can generate four CP end-fire radiation beams with beam-switching in horizontal plane has been designed, fabricated, and measured. The impedance and isolation bandwidth from 57.8 to 62.5 GHz, stable LHCP radiation beams, and gain up to 11.01 dBic were achieved. The simulated and measured results agree with each other, and show that the proposed CP multi-beam array would be an attractive candidate to the future short-range millimeter-wave wireless communication.

REFERENCES

[1] A. F. Boccardi, R. W. Heath, Jr., A. Lozano, T. L. Marzetta, and P. Popovski, "Five disruptive technology directions for 5G," *IEEE commun. Mag.*, vol. 52, no. 2, pp. 80–94, Feb. 2014.

[2] P. Wang, Y. Li, L. Song, and B. Vucetic, "Multi-gigabit millimeter wave wireless communications for 5G: From fixed access to cellular networks," *IEEE Commun. Mag.*, vol. 53, no. 1, pp. 168–178, Jan. 2015.

[3] J. Ala-Laurinaho *et al.*, "2-D beam-steerable integrated lens antenna system for 5G *E*-band access and Backhaul," *IEEE Trans. Microw. Theory Techn.*, vol. 64, no. 7, pp. 2244–2255, Jul. 2016.

[4] W. Hong *et al.*, "Multibeam antenna technologies for 5G wireless communications," *IEEE Trans. Antennas Propag.*, vol. 65, no. 12, pp. 6231–6249, Dec. 2017.

[5] K. Tekkouk, J. Hirokawa, R. Sauleau, M. Ettorre, M. Sano, and M. Ando, "Dual-layer ridged waveguide slot array fed by a butler matrix with sidelobe control in the 60-GHz band," *IEEE Trans. Antennas Propag.*, vol. 63, no. 9, pp. 3857–3867, Sep. 2015.

[6] K. Tekkouk, M. Ettorre, L. Le Coq, and R. Sauleau, "Multibeam SIW slotted waveguide antenna system fed by a compact dual-layer Rotman lens," *IEEE Trans. Antennas Propag.*, vol. 64, no. 2, pp. 504–514, Feb. 2016.

[7] T. Djerafi and K. Wu, "A low-cost wideband 77-GHz planar butler matrix in SIW technology," *IEEE Trans. Antennas Propag.*, vol. 60, no. 10, pp. 4949–4954, Oct. 2012.

[8] L.-H. Zhong, Y.-L. Ban, J.-W. Lian, Q.-L. Yang, J. Guo, and Z.-F. Yu, "Miniaturized SIW multibeam antenna array fed by dual-layer 8×8 butler matrix," *IEEE Antennas Wireless Propag. Lett.*, vol. 16, pp. 3018–3021, 2017.

[9] P. Chen *et al.*, "A multibeam antenna based on substrate integrated waveguide technology for MIMO wireless communications," *IEEE Trans. Antennas Propag.*, vol. 57, no. 6, pp. 1813–1821, Jun. 2009.

[10] J. Wang, Y. Li, L. Ge, J. Wang, and K.-M. Luk, "A 60 GHz horizontally polarized magnetoelectric dipole antenna array with 2-D multibeam endfire radiation," *IEEE Trans. Antennas Propag.*, vol. 65, no. 11, pp. 5837–5845, Nov. 2017.

[11] W. Yang, Y. Yang, W. Che, C. Fan, and Q. Xue, "94-GHz compact 2-D multibeam LTCC antenna based on multifolded SIW beam-forming network," *IEEE Trans. Antennas Propag.*, vol. 65, no. 8, pp. 4328–4333, Aug. 2017.

[12] T. Manabe *et al.*, "Polarization dependence of multipath propagation and high-speed transmission characteristics of indoor millimeter-wave channel at 60 GHz," *IEEE Trans. Veh. Technol.*, vol. 44, no. 2, pp. 268–274, May 1995.

[13] Y. Zhao and K.-M. Luk, "Dual circular-polarized SIW-fed high-gain scalable antenna array for 60 GHz applications," *IEEE Trans. Antennas Propag.*, vol. 66, no. 3, pp. 1288–1298, Mar. 2017.

[14] Y. J. Cheng, X. Y. Bao, and Y. X. Guo, "60-GHz LTCC miniaturized substrate integrated multibeam array antenna with multiple polarizations," *IEEE Trans. Antennas Propag.*, vol. 61, no. 12, pp. 5958–5967, Dec. 2013.

[15] Q. Wu, J. Hirokawa, J. Yin, C. Yu, H. Wang, and W. Hong, "Millimeter-wave planar broadband circularly polarized antenna array using stacked curl elements," *IEEE Trans. Antennas Propag.*, vol. 65, no. 12, pp. 7052–7062, Dec. 2017.

[16] W. Hong, K.-H. Baek, Y. Lee, Y. Kim, and S.-T. Ko, "Study and prototyping of practically large-scale mmWave antenna systems for 5G cellular devices," *IEEE Commun. Mag.*, vol. 52, no. 9, pp. 63–69, Sep. 2014.

[17] Y. Li and K.-M. Luk, "A multibeam end-fire magnetoelectric dipole antenna array for millimeter-wave applications," *IEEE Trans. Antennas Propag.*, vol. 64, no. 7, pp. 2894–2904, Jul. 2016.

[18] Y. Liu *et al.*, "Millimeterwave and terahertz waveguide-fed circularly polarized antipodal curvedly tapered slot antennas," *IEEE Trans. Antennas Propag.*, vol. 64, no. 5, pp. 1607–1614, May 2016.

[19] Y. Yao, X. Cheng, J. Yu, and X. Chen, "Analysis and design of a novel circularly polarized antipodal linearly tapered slot antenna," *IEEE Trans. Antennas Propag.*, vol. 64, no. 10, pp. 4178–4187, Oct. 2016.

[20] X. Cheng, Y. Yao, Z. Chen, J. Yu, and X. Chen, "Compact wideband circularly polarized antipodal curvedly tapered slot antenna," *IEEE Antennas Wireless Propag. Lett.*, vol. 17, no. 4, pp. 666–669, Apr. 2018.

[21] X. Cheng *et al.*, "Analysis and design of a wideband end-fire circularly polarized septum antenna," *IEEE Trans. Antennas Propag.*, to be published. [Online]. Available: https://ieeexplore.ieee.org/document/8444448, doi: 10.1109/TAP.2018.2866584.

[22] Q. Wu, J. Hirokawa, J. Yin, C. Yu, H. Wang, and W. Hong, "Millimeter-wave multibeam endfire dual-circularly polarized antenna array for 5G wireless applications," *IEEE Trans. Antennas Propag.*, vol. 66, no. 9, pp. 4930–4935, Sep. 2018.

[23] N. Bayat-Makou and A. A. Kishk, "Contactless air-filled substrate integrated waveguide," *IEEE Trans. Microw. Theory Techn.*, vol. 66, no. 6, pp. 2928–2935, Jun. 2018.

XIAOHE CHENG (S'17) received the B.Sc. degree from Hebei Univerisity, Baoding, China, in 2014. He is currently pursuing the Ph.D. degree in electronics and communication engineering at the Beijing University of Posts and Telecommunications, Beijing, China. Since 2017, he has been a Junior Visiting Fellow with the Ando and Hirokawa Laboratory, Tokyo Institute of Technology, Tokyo, Japan.

His current research interests include wideband antennas, circularly polarized antenna, and high-gain millimeter-wave antennas.

YUAN YAO (M'11–SM'15) received the B.Sc. degree in communication engineering from Tianjin University, China, in 2004, and the Ph.D. degree in electronic science and technology from Tsinghua University, China, in 2010.

In 2010, he joined the School of Electronic Engineering, Beijing University of Posts and Telecommunications, where he is currently a Full Professor. He has published over 100 papers and three books. His research interests include the fields of antennas, RFID, and THz technology.

Prof. Yao is currently an Editor of the *International Journal of Antennas and Propagation* and also a Reviewer of the IEEE TRANSACTIONS ON ANTENNAS AND PROPAGATION.

TAKASHI TOMURA (S'11–M'14) was born in Sendai, Japan. He received the B.S., M.S., and D.E. degrees in electrical and electronic engineering from the Tokyo Institute of Technology, Tokyo, Japan, in 2008, 2011, and 2014, respectively. He was a Research Fellow of the Japan Society for the Promotion of Science in 2013. From 2014 to 2017, he was at Mitsubishi Electric Corporation, Tokyo, and was engaged in research and development of aperture antennas for satellite communications and radar systems. He is currently a Specially Appointed Assistant Professor at the Tokyo Institute of Technology. His research interests include electromagnetic analysis, aperture antennas, and planar waveguide slot array antennas.

Dr. Tomura is a member of the IEICE. He received the Best Student Award from Ericsson, Japan, in 2012, and the IEEE AP-S Tokyo Chapter Young Engineer Award in 2015.

JIRO HIROKAWA (S'89–M'90–SM'03–F'12) received the B.S., M.S., and D.E. degrees in electrical and electronic engineering from the Tokyo Institute of Technology (Tokyo Tech), Tokyo, Japan, in 1988, 1990, and 1994, respectively.

He was a Research Associate from 1990 to 1996 and an Associate Professor from 1996 to 2015 at Tokyo Tech, where he is currently a Professor. He was with the Antenna Group, Chalmers University of Technology, Gothenburg, Sweden, as a Post-Doctoral Fellow, from 1994 to 1995. His research area has been in slotted waveguide array antennas and millimeter-wave antennas. He is a fellow of IEICE. He received the IEEE AP-S Tokyo Chapter Young Engineer Award in 1991, the Young Engineer Award from IEICE in 1996, the Tokyo Tech Award for Challenging Research in 2003, the Young Scientists' Prize from the Minister of Education, Cultures, Sports, Science and Technology, Japan, in 2005, the Best Paper Award in 2007 and the Best Letter Award in 2009 from the IEICE Communications Society, and the IEICE Best Paper Award in 2016.

TAO YU received the B.E. degree in communication engineering from the Taiyuan Institute of Technology, China, in 2008, and the M.E. degree in signal and information processing from the Communication University of China in 2010, and the Dr.Eng. degree from the Tokyo Institute of Technology in 2017. Since 2012, he joined the Sakaguchi Lab, Department of Electrical and Electronic Engineering, Tokyo Institute of Technology, Japan, where he is currently a Post-Doctoral Researcher with the Sakaguchi Lab. His research interests are sensor networks, localization, distributed control and building energy management. He is a member of IEICE.

JUNSHENG YU received the B.Sc. degree in physics from the Fuyang Teachers College, China, in 1983, the M.S. degree in physical electronics from the Southwestern Institute of Physics, China, in 1986, and the Ph.D. degree in electronic physics and devices from the University of Electronic Science and Technology of China, Chengdu, in 1990.

In 2003, he joined the School of Electronic Engineering, Beijing University of Posts and Telecommunications, where he is currently a Full Professor. He has published dozens of papers. His research area is focused on microwave and millimeter wave theory, THz system, and physical electronics. He received the Royal Society Scholarship in 1993 and did his visiting research at Abreu Thai Dundee University and the Imperial College University of London.

Dr. Yu is currently a member of experts group of the national high technology research and development program of China.

XIAODONG CHEN (M'96–SM'07–F'14) received the B.Sc. degree in electronic engineering from Zhejiang University, Hangzhou, China, in 1983 and the Ph.D. degree in microwave electronics from the University of Electronic Science and Technology of China, Chengdu, in 1988.

In 1988, he joined the Department of Electronic Engineering, King's College, University of London, as a Post-Doctoral Visiting Fellow. In 1990, he was with the King's College as a Research Associate and was appointed to an EEV Lectureship later on. In 1999, he joined the School of Electronic Engineering and Computer Science, Queen Mary University of London, where is currently a Professor at the School of Electronic Engineering and Computer Science. He has authored and co-authored over 300 publications. His research interests include in the fields of wireless communications, microwave devices, and antennas.

Dr. Chen is currently a member of the UK EPSRC Review College and a Technical Panel of the IET Antennas and Propagation Professional Network.